Physical Review E (accepted on 21 August 2014)

Accurate control of hyperbolic trajectories in any dimension

Sanjeeva Balasuriya*
School of Mathematical Sciences, University of Adelaide, SA 5005, Australia

Kathrin Padberg-Gehle†
Institute of Scientific Computing, Technische Universität Dresden, D-01062 Dresden, Germany
(Dated: September 2, 2014)

The unsteady (nonautonomous) analogue of a hyperbolic fixed point is a hyperbolic trajectory, whose importance is underscored by its attached stable and unstable manifolds, which have relevance in fluid flow barriers, chaotic basin boundaries and the long-term behaviour of the system. We develop a method for obtaining the unsteady control velocity which forces a hyperbolic trajectory to follow a user-prescribed variation with time. Our method is applicable in any dimension, and accuracy to any order is achievable. We demonstrate and validate our method by (i) controlling the fixed point at the origin of the Lorenz system, for example obtaining a user-defined nonautonomous attractor, and (ii) the saddle points in a droplet flow, using localised control which generates global transport.

PACS numbers: 02.30.Yy, 02.30.Hq, 47.85.L-, 05.45.Gg, 47.10.Fg

I. INTRODUCTION

The concept of hyperbolic trajectories in ordinary differential equations encapsulates a range of entities which have a strong influence in governing global motion. Hyperbolic trajectories include: (i) Saddle fixed points of steady flows, which have attached to them both a stable and an unstable manifold; (ii) Fixed points of steady flows which are attracting; (iii) Fixed points of steady flows which are repelling; (iv) Specialised trajectories of *unsteady* flows which have attached to them both a stable and an unstable manifold; and (v) Specialised trajectories of unsteady flows which have a full-dimensional stable or an unstable manifold. For fixed points of steady flows, hyperbolicity is expressed by the linearised Jacobian matrix evaluated at the fixed point having no eigenvalues on the imaginary axis. For more general situations, hyperbolicity needs to be defined in terms of the computationally difficult *exponential dichotomy* conditions [1–4] (see Appendix A). It must be emphasised that hyperbolic trajectories in unsteady flows cannot be determined by considering instantaneous fixed points [5]; neither are instantaneous eigenvalues useful. The importance of the large class of hyperbolic trajectories outlined above is underscored by their effect on the *global* behaviour. For example, it is well-known that stable and unstable manifolds form important flow separators in fluid flows, thereby providing a skeleton which distinguishes between regions of anomalous motion [4, 6–10, e.g.]. Hyperbolic trajectories are entities to which these stable and unstable manifolds are attached, and hence their motion with time governs the time-variation of these flow separators. A different example comes from hyperbolic trajectories which are purely attracting, i.e., they have a full-dimensional stable manifold, but no unstable manifold attached to them. While these may also move around in phase space in unsteady flows, they nevertheless are the entities to which all nearby initial conditions get attracted as time progresses. Thus, such hyperbolic trajectories govern the eventual behaviour of the system.

The ability to *control* the time-varying behaviour of hyperbolic trajectories can therefore have tremendous applications across a range of areas. A classical example from fluid mechanics is the concept of a fluidic device which achieves droplet manipulation through positioning at the hyperbolic trajectory location [11–24]. In the paradigmatic two-dimensional device with a hyperbolic point with attached one-dimensional stable and unstable manifolds, droplet elongation in the unstable direction is achieved by this process. For droplets travelling within an unsteady flow (such as nano/microdroplets currently under intensive investigation for their promise in processing single cells [25, cf.]), such elongation can be achieved by positioning the droplet at a hyperbolic trajectory location, whose control is therefore desirable. While the hyperbolic trajectory described above is exterior to the droplet, many droplet models in the literature themselves possess on the droplet's surface a saddle-like hyperbolic trajectory [26–36, e.g.] whose motion influences intra-droplet chaotic transport because its attached stable and unstable manifolds undergo nontrivial motion. There is currently only one method in the scientific literature which can control manifold paths [37], but it is limited to two-dimensional nearly steady flows with one-dimensional stable/unstable manifolds. In the quest for controlling manifolds in n-dimensions, a first step would be to force the hyperbolic trajectory (to which these manifolds are attached) to follow a prescribed motion. By

* sanjeevabalasuriya@yahoo.com
† kathrin.padberg@tu-dresden.de

causing a time-varying movement of the hyperbolic trajectory using a *localised* control, it will be possible to impact *global* behaviour, since the global manifolds are slaved to these hyperbolic trajectories. Thus, if hyperbolic trajectories with a heteroclinic manifold connecting them are made to move in a judiciously chosen manner, it will be possible to break apart the heteroclinic manifold into intersecting stable and unstable manifolds, thereby causing complicated (i.e., chaotic) mixing. Thus, controlling hyperbolic trajectories is a yet-unexplored avenue in the topic of controlling and optimising mixing which is eliciting much recent interest [23, 24, 38–50, e.g.].

In fluid mechanics, the phase space of the ordinary differential equations governing particle motion is the physical space itself. Hyperbolic trajectories also have a profound influence in more *general* phase spaces, since once again stable and unstable manifolds form separators, for example in demarcating basin boundaries of chaotic or nonchaotic attractors. Purely attracting hyperbolic trajectories are particularly important, since they govern the long-term evolution of the system. If such a hyperbolic trajectory could be moved around in a *user-specified* fashion, then the the global system's eventual behaviour could be *specified*. In particular, this will allow the long-term behaviour to be made *time-varying* in a desired fashion; essentially, trajectories will approach a user-specified *nonautonomous attractor*. Such a method would extend more classical control strategies which, for example, attempt to have a chaotic system approach a *fixed* point [51–55], a periodic orbit [56–61] or even a chaotic regime [62] by taking advantage of the relevant entity's stable manifold.

Despite the potential applications, a theory for achieving precisely this control—ensuring that hyperbolic trajectories follow user-specified time-variation—has not yet been developed, except for in a fairly limited situation by us [63]. In this recent work, we achieved hyperbolic trajectory control using a perturbative method in two-dimensions [63], but in this article we provide a method of achieving *any* order of accuracy, in *any* dimension. This novel technique comes from a very different approach to classical chaos control theory [51, 57, 64]; we are controlling the motion of an important entity in phase space, and not attempting to stabilise an unstable trajectory.

We describe our method in Section II. We take advantage of the specialised behaviour of hyperbolic trajectories—namely, attracting and/or repelling nearby trajectories—to construct a bootstrapping process for determining increasingly accurate control velocities for achieving desired hyperbolic trajectory motion. In Section III, we apply the method to find the control velocity which moves the origin—a hyperbolic fixed point—of the Lorenz system [65] to a hyperbolic trajectory which follows *prescribed* motion. For example, we can ensure the system has a globally attracting trajectory which follows *user-specified* time-variation when $\rho < 1$. An important extension to known methods is that with our method this attracting hyperbolic trajectory can be made to move around in a time-varying fashion as specified by us, as opposed to the more standard situation of attempting to control a chaotic system to reach a *fixed* point [51, 53, 54]. We numerically verify the excellent accuracy of our method. For a highly chaotic parameter regime in which the hyperbolic trajectory has *both* a stable and an unstable manifold, we demonstrate that we can achieve both a time-periodic and a time-aperiodic behaviour of a hyperbolic trajectory, again with the time-variation following our specifications. Thus, we are able to control a significant feature in a highly chaotic system. In Section IV, we apply the control method to the fluid dynamical example of a 'two-cell' droplet [31, 32, 35, 36, 66], which is the Hadamard-Rybczynski solution to a three-dimensional Stokes flow problem. This model has importance in the quest for improving mixing within microdroplets [31, 32, 35, 36, 66], which can be achieved by breaking the invariant manifolds and causing them to intersect in complicated ways. We show how we can make the hyperbolic trajectories at the north and south poles to move *independently*, according to our specifications which are designed to make their stable and unstable manifolds mingle to achieve good intra-droplet transport. We show in Section IV that we can achieve such control to high accuracy, and demonstrate the resulting fluid transport.

The control method we have developed works for ordinary differential equations in any dimension, and moreover we can achieve arbitrarily good accuracy by utilising Taylor expansions to as high an order as we like, as explained in Section II. As such, this forms a powerful method for controlling significant flow-governing structures in chaotic and nonchaotic systems, which we anticipate to be tremendously useful across many disciplines.

II. CONTROL VELOCITY DETERMINATION

We consider the uncontrolled system

$$\dot{\boldsymbol{x}} = \boldsymbol{u}(\boldsymbol{x}, t) \tag{1}$$

for $\boldsymbol{x} \in \Omega \subseteq \mathbb{R}^n$, $n \geq 2$, in which $\boldsymbol{u}$ is sufficiently smooth [67]. We assume that $\boldsymbol{u}(\boldsymbol{x}, t)$ is fully known, and that a hyperbolic trajectory $\boldsymbol{x}^{(0)}(t)$ of (1) is also known. Thus, our method applies to situations in which the details of the uncontrolled system are known in full detail, and our intention is to determine a control velocity such that the hyperbolic trajectory could be moved with time according to our wishes.

The hyperbolic trajectory $\boldsymbol{x}^{(0)}(t)$ could be *any* of the entities outlined in the first paragraph of the introduction; the intuition is that it is a (potentially time-varying) trajectory of (1), which possesses an m-dimensional stable manifold and an $(n-m)$-dimensional unstable manifold with $m \in \{0, 1, 2, 3, , \cdots, n\}$. This informal statement of a hyperbolic trajectory in a nonautononous system may be formally clarified in terms of exponential dichotomies; see Appendix A.

The implication of the definition of hyperbolicity is that there is a tubular neighbourhood $\mathcal{V}_t := \mathcal{U}_t \times \mathbb{R}$ in which $\mathcal{U}_t \subset \Omega$ is an open neighbourhood of $\boldsymbol{x}^{(0)}(t)$ at each time t, such that the *only* trajectory of $\dot{\boldsymbol{x}} = \boldsymbol{u}(\boldsymbol{x}, t), \dot{t} = 1$ which remains within $\mathcal{V}_t$ in both backwards and forwards time is $\left(\boldsymbol{x}^{(0)}(t), t\right)$. This is because if there is a stable manifold (if $m > 0$), then in backwards time nearly all nearby trajectories will get pulled away from $\boldsymbol{x}^{(0)}(t)$ due to its influence. The only exceptions to this are trajectories which lie precisely on the unstable manifold, which will get attracted towards the hyperbolic trajectory. Thus, if there is a stable manifold, then all trajectories which are not on the unstable manifold exit $\mathcal{V}_t$ as $t \to -\infty$. Conversely, if there is an unstable manifold (if $m < n$), then all trajectories which are not on the stable manifold exit $\mathcal{V}_t$ as $t \to \infty$. It is therefore only trajectories which are on *both* the stable and the unstable manifold which remain within $\mathcal{V}_t$ for all $t \in \mathbb{R}$. This is trivially the set $\left(\boldsymbol{x}^{(0)}(t), t\right)$ itself. We note that this statement is still true even if one or the other of the stable or unstable manifold did not exist, that is, if $m = 0$ or $m = n$.

We now plan to impose a control velocity $\boldsymbol{v}$ leading to the system

$$\dot{\boldsymbol{x}} = \boldsymbol{u}(\boldsymbol{x}, t) + \boldsymbol{v}(\boldsymbol{x}, t, \varepsilon)\,, \tag{2}$$

in which the parameter $\varepsilon \in \mathcal{I} = (-\varepsilon_0, \varepsilon_0)$ for ε_0 is sufficiently small, and that control velocity satisfies $\boldsymbol{v}(\boldsymbol{x}, t, 0) = \boldsymbol{0}$ and is sufficiently smooth [68]. We address the following: How does one choose the control velocity $\boldsymbol{v}$ in order to ensure that a *specified* $\boldsymbol{x}(t, \varepsilon)$ is a hyperbolic trajectory of (2)? (We note that by the roughness of exponential dichotomies [1, 69, 70], the hyperbolic trajectory persists for small ε_0.)

Before we proceed with our control velocity determination, we remark that the instance in which $m = n$ (i.e., the stable manifold of $\boldsymbol{x}^{(0)}(t)$ is full-dimensional, and hence forms an attractor) is particularly interesting. In this case, a nearby attractor persists under perturbation [71]. This attractor is of course the perturbed hyperbolic trajectory. By our process, we can *prescribe* this attractor's time-variation.

We now turn to determining the control in the general instance where $0 \leq m \leq n$, that is, the stable manifold may be zero-dimensional, an intermediate dimension, or full-dimensional. These correspond to the unperturbed hyperbolic trajectory being a repeller, having saddle-like structure, or being an attractor, respectively. Now, by continuity in ε, the desired hyperbolic trajectory path $\boldsymbol{x}(t, \varepsilon)$ must satisfy the condition $\boldsymbol{x}(t, 0) = \boldsymbol{x}^{(0)}(t)$. Since $\boldsymbol{x}(t, \varepsilon)$ is required to be a hyperbolic trajectory of (2) and is ε-close to $\boldsymbol{x}^{(0)}(t)$, it too inherits a tubular neighbourhood $\mathcal{V}_t(\varepsilon)$ to which the only trajectory confined for $t \in \mathbb{R}$ is $(\boldsymbol{x}(t, \varepsilon), t)$. Within $\mathcal{V}_t(\varepsilon)$ we define

$$x_i^{(j)}(t) := \frac{1}{j!}\,\frac{\partial^j x_i}{\partial \varepsilon^j}(t, 0) \tag{3}$$

in which the subscript $i \in \{1, 2, \cdots, n\}$ identifies the component of $\boldsymbol{x}$, and the superscript $j \in \{0, 1, \cdots\}$ is the order of the ε-derivative. That is, each component of $\boldsymbol{x}$ possesses a Taylor expansion

$$x_i(t, \varepsilon) = x_i^{(0)}(t) + \varepsilon x_i^{(1)}(t) + \varepsilon^2 x_i^{(2)}(t) + \varepsilon^3 x_i^{(3)}(t) + \cdots \tag{4}$$

in which the coefficients are known to as high an order as needed. Since $\boldsymbol{x}(t, \varepsilon)$ is the *only* trajectory which remains within $\mathcal{V}_t(\varepsilon)$ in both backwards and forwards time, if this Taylor expansion is considered valid for all times, it *must* represent exactly a hyperbolic trajectory. Thus, (4) unambiguously represents the perturbed hyperbolic trajectory, and not just any other trajectory in the flow. To find the control velocity $\boldsymbol{v}$, we express it in terms of its Taylor expansion

$$v_i(\boldsymbol{x}, t, \varepsilon) = \varepsilon v_i^{(1)}(\boldsymbol{x}, t) + \varepsilon^2 v_i^{(2)}(\boldsymbol{x}, t) + \varepsilon^3 v_i^{(3)}(\boldsymbol{x}, t) + \cdots\,. \tag{5}$$

We will show how to determine the coefficients of (5) in a step-by-step fashion in terms of the known quantities, namely $\boldsymbol{u}(\boldsymbol{x}, t)$ and the coefficients $x_i^{(0)}(t)$, $x_i^{(1)}(t)$, $x_i^{(2)}(t)$, etc.

Consider the ith component of (2). Substituting the Taylor expansions (4) and (5) into (2) leads to

$$\begin{aligned}
&\dot{x}_i^{(0)} + \varepsilon \dot{x}_i^{(1)} + \varepsilon^2 \dot{x}_i^{(2)} + \mathcal{O}(\varepsilon^3) = u_i \\
&+ \left(\varepsilon x_j^{(1)} \frac{\partial u_i}{\partial x_j} + \varepsilon^2 x_j^{(2)} \frac{\partial u_i}{\partial x_j} + \frac{\varepsilon^2}{2} x_j^{(1)} x_k^{(1)} \frac{\partial^2 u_i}{\partial x_j \partial x_k} \right) \\
&+ \left(\varepsilon v_i^{(1)} + \varepsilon^2 x_j^{(1)} \frac{\partial v_i^{(1)}}{\partial x_j} \right) + \varepsilon^2 v_i^{(2)} + \mathcal{O}(\varepsilon^3)
\end{aligned} \tag{6}$$

for each component i. Here, each of the quantities on the right is evaluated on the hyperbolic trajectory $\left(\boldsymbol{x}^{(0)}(t), t\right)$ of (1), and the Einstein summation convention has been used; when a sub/superscript is repeated, it is assumed that these are summed over for each term. Separating out the order ε^0 term yields the self-consistent fact from the uncontrolled system that

$$\dot{x}_i^{(0)}(t) = u_i \left(\boldsymbol{x}^{(0)}(t), t \right)\,. \tag{7}$$

Now, the order ε and ε^2 terms of (6) are respectively

$$v_i^{(1)} \left(\boldsymbol{x}^{(0)}(t), t \right) = \dot{x}_i^{(1)}(t) - x_j^{(1)}(t) \frac{\partial u_i}{\partial x_j} \left(\boldsymbol{x}^{(0)}(t), t \right)\,; \tag{8}$$

$$\begin{aligned}
v_i^{(2)} \left(\boldsymbol{x}^{(0)}(t), t \right) = {} & \dot{x}_i^{(2)}(t) - x_j^{(2)}(t) \frac{\partial u_i}{\partial x_j} \left(\boldsymbol{x}^{(0)}(t), t \right) \\
& - \frac{1}{2} x_j^{(1)}(t) x_k^{(1)}(t) \frac{\partial^2 u_i}{\partial x_j \partial x_k} \left(\boldsymbol{x}^{(0)}(t), t \right) \\
& - x_j^{(1)}(t) \frac{\partial v_i^{(1)}}{\partial x_j} \left(\boldsymbol{x}^{(0)}(t), t \right)\,.
\end{aligned} \tag{9}$$

These give requirements for $v_i^{(1,2)}$ only on the unperturbed hyperbolic trajectory $\left(\boldsymbol{x}^{(0)}(t), t\right)$; any smooth extension to Ω is permissible. We note however that (9)

does not express $v_i^{(2)}$ in terms of known quantities, because of the derivative $\partial v_i^{(1)}/\partial x_j$. The resolution is to choose $v_i^{(1)}$ to be globally given by

$$v_i^{(1)}(\boldsymbol{x},t) = \dot{x}_i^{(1)}(t) - x_j^{(1)}(t)\frac{\partial u_i}{\partial x_j}(\boldsymbol{x},t)\ , \qquad (10)$$

thereby satisfying (8). Differentiating (10) with respect to a component x_k gives

$$\frac{\partial v_i^{(1)}}{\partial x_k}(\boldsymbol{x},t) = -x_j^{(1)}\frac{\partial^2 u_i}{\partial x_j \partial x_k}(\boldsymbol{x},t)\ , \qquad (11)$$

which can be substituted into (9). The last two terms in (9) are then seen to be of the same type, and can be combined. The condition on $v_i^{(2)}$ in (9) would only be needed on the unperturbed hyperbolic trajectory $\big(\boldsymbol{x}^{(0)}(t),t\big)$; we once again replace this with $(\boldsymbol{x},t)$ to be consistent to (9). This gives us the choice for the second-order component of the velocity field to be

$$v_i^{(2)}(\boldsymbol{x},t) = \dot{x}_i^{(2)}(t) - x_j^{(2)}(t)\frac{\partial u_i}{\partial x_j}(\boldsymbol{x},t) + \frac{1}{2}x_j^{(1)}(t)x_k^{(1)}(t)\frac{\partial^2 u_i}{\partial x_j \partial x_k}(\boldsymbol{x},t)\ . \qquad (12)$$

Following this procedure for the third-order in ε term in (5) (calculations not shown) eventually leads to

$$v_i^{(3)}(\boldsymbol{x},t) = \dot{x}_i^{(3)}(t) - x_j^{(3)}(t)\frac{\partial u_i}{\partial x_j}(\boldsymbol{x},t) + x_j^{(1)}(t)x_k^{(2)}(t)\frac{\partial^2 u_i}{\partial x_j \partial x_k}(\boldsymbol{x},t) - \frac{1}{6}x_j^{(1)}(t)x_k^{(1)}(t)x_l^{(1)}(t)\frac{\partial^3 u_i}{\partial x_j \partial x_k \partial x_l}(\boldsymbol{x},t) \qquad (13)$$

Thus, by choosing the velocity field in the form (5) subject to (10), (12) and (13), one can ensure that a hyperbolic trajectory of (2) follows the path $\boldsymbol{x}(t,\varepsilon)$, correct to $\mathcal{O}(\varepsilon^3)$. By continuing this process, the control velocity can be determined to as high an order of ε as required; we stop here for brevity.

We will make several remarks about this technique. First, if incompressibility were a necessity in the flow (as might be necessary in a fluidic application), the control velocities in (10), (12) and (13) will automatically inherit the incompressibility of the base velocity $\boldsymbol{u}$. Second, if our intention was to simultaneously control *several* hyperbolic trajectories in a system, we can do so by using the computed velocity components locally near each of the trajectories, while switching them off when further away to avoid disrupting the control of the other hyperbolic trajectories. Third, when the method is stopped at some order (say ε^m), then the error would be bounded by $C(t)\varepsilon^{m+1}$ for some function $C(t)$ which may grow as $t \to \pm\infty$, and so it should be borne in mind that the error may grow with time [72].

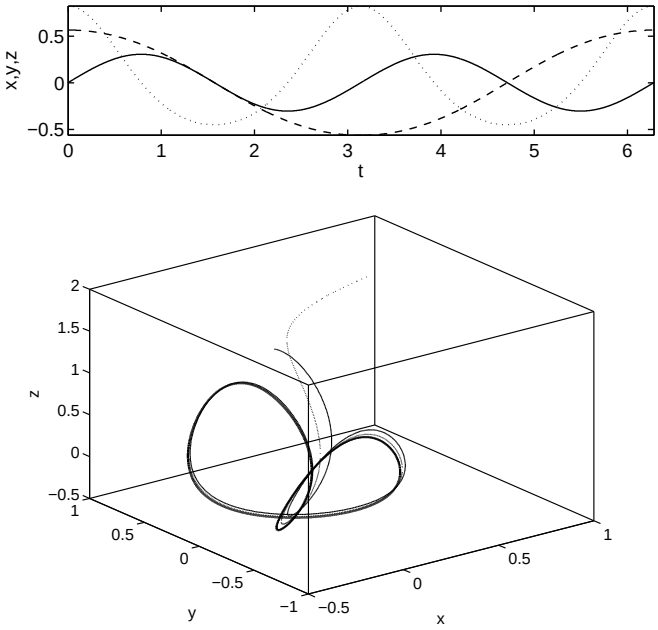

FIG. 1. Periodic hyperbolic trajectory $\boldsymbol{x}_{(p)}$ for $\varepsilon = 0.6$ as defined by (15) over time interval $[0, 2\pi]$, with (x, y, z) represented by solid, dashed and dotted curves respectively (top panel). Solution curves (dotted and solid) of two initial conditions approaching the trajectory $\boldsymbol{x}_{(p)}(t)$ (thick curve) in phase space (bottom panel).

III. LORENZ SYSTEM

For our uncontrolled system (1), we take

$$\dot{x} = \sigma(y-x)\ ,\ \dot{y} = x(\rho - z) - y\ ,\ \dot{z} = xy - \beta z\ , \qquad (14)$$

the classical Lorenz system [65]. We first examine the parameter regime $\rho = 0.5$, $\sigma = 10$ and $\beta = 8/3$, at which (14) has an attracting fixed point at the origin. Rather than the system approaching a fixed point, suppose we would like it to approach some nonautonomous entity of interest to us. As an example, we choose a periodic trajectory

$$\boldsymbol{x}_{(p)}(t) = \begin{pmatrix}0\\0\\0\end{pmatrix} + \begin{pmatrix}\sinh\left[\varepsilon \sin t \cos t\right]\\ \sin\left[\varepsilon\cos t\right]\\ e^{\varepsilon\cos 2t} - 1\end{pmatrix}\ , \qquad (15)$$

with $\varepsilon = 0.6$. A plot of this trajectory is shown in Fig. 1. Thus, we are specifying an attractor for the Lorenz system, and want to determine the control velocity which results in all nearby trajectories going to this attractor. (In this instance, *all* global trajectories will go to this attractor since the original attractor was globally attracting; in general, however, our method can only fully guarantee persistence of attraction locally.) By Taylor expanding

$\boldsymbol{x}_{(p)}(t)$ in ε we obtain

$$\boldsymbol{x}_{(p)}(t) = \begin{pmatrix}0\\0\\0\end{pmatrix} + \varepsilon \begin{pmatrix}\sin t\cos t\\ \cos t\\ \cos 2t\end{pmatrix} + \frac{\varepsilon^2}{2}\begin{pmatrix}0\\0\\ \cos^2 2t\end{pmatrix} + \frac{\varepsilon^3}{6}\begin{pmatrix}\cos^3 t\sin^3 t\\ -\cos^3 t\\ \cos^3 2t\end{pmatrix} + \mathcal{O}(\varepsilon^4)\,, \quad (16)$$

which, consistent with (4), becomes the uncontrolled fixed point $(0,0,0)$ when $\varepsilon = 0$. Upon substitution into equations (10), (12) and (13), we get

$$\boldsymbol{v}^{(1)}_{(p)}(\boldsymbol{x},t) = \begin{pmatrix}\cos 2t + \sigma\cos t(\sin t - 1)\\ -(1+(\rho - z)\cos t)\sin t + \cos t + x\cos 2t\\ -2\sin 2t - y\sin t\cos t - x\cos t + \beta\cos 2t\end{pmatrix},$$

$$\boldsymbol{v}^{(2)}_{(p)}(\boldsymbol{x},t) = \begin{pmatrix}0\\ \frac{x}{2}\cos^2 2t - \sin t\cos t\cos 2t\\ -2\sin 2t\cos 2t + \frac{\beta}{2}\cos^2 2t + \sin t\cos^2 t\end{pmatrix},$$

$$\boldsymbol{v}^{(3)}_{(p)}(\boldsymbol{x},t) = \frac{1}{2}\begin{pmatrix}\sin^2 t\cos^2 t\cos 2t\\ \sin t\cos t(\cos t - \cos^2 2t)\\ -2\cos^2 2t\sin 2t\end{pmatrix} + \frac{1}{6}\begin{pmatrix}\sigma\cos^3 t(\sin^3 t + 1)\\ -((\rho - z)\sin^3 t + 1)\cos^3 t + x\cos^2 2t\\ \cos^3 t\left(x - y\sin^3 t\right) + \beta\cos^3 2t\end{pmatrix}.$$

The above defines the required control velocity (5) to $\mathcal{O}(\varepsilon^3)$. In the bottom plot of Fig. 1, we show the evolution of two arbitrary initial conditions to the controlled system (dotted and solid curves); they both approach the desired periodic trajectory (15), as shown by the thick figure-8 like curve, as desired. This occurs for *any* chosen initial condition for the controlled system. Thus, we have managed to specify the nonautonomous attractor to our system. By putting in any behaviour we require for our $\boldsymbol{x}(t)$, we are thus able to obtain *any* specified bounded long-term behaviour of the system.

We next consider $\sigma = 10$, $\beta = 8/3$ and $\rho = 28$, the classical parameter values [65] at which the Lorenz system is known to possess a chaotic attractor [73]. The origin is now a saddle point, and possesses a two-dimensional stable manifold and a one-dimensional unstable manifold, which have a profound influence on how trajectories evolve. For example, trajectories cannot cross the stable manifold, which is therefore a separating surface. Since in the chaotic regime, the stable manifold exhibits great complexity, but can be characterised in a neighbourhood near $(0,0,0)$ using standard dynamical systems techniques: locally, it is tangential to the plane defined by the tangent vectors $(0,0,1)$ and $(9+\sqrt{1201}, -56, 0)$. Classical chaos control methods attempt to stabilise the saddle point by pushing trajectories onto its stable manifold, away from the influence of the destabilising unstable manifold [51, e.g.]. Here, we do not attempt to control the chaos inherent in the system, but rather to control the *location* of the hyperbolic entity (which was at $(0,0,0)$ in the absence of a control) at which the stable and unstable manifolds originate. Through an imposed control velocity, we will move this hyperbolic fixed point to, first, the periodic hyperbolic trajectory (15), and second, to a quasi-periodic hyperbolic trajectory

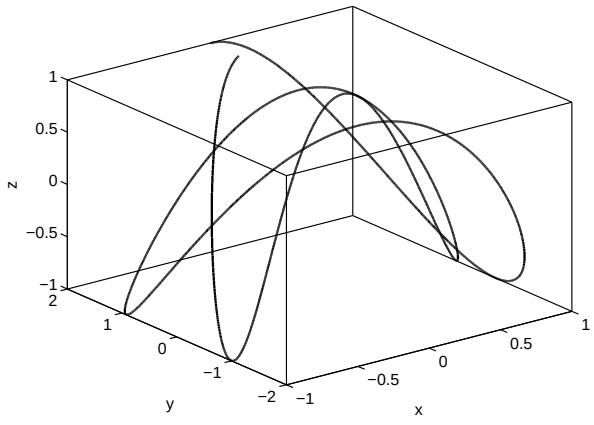

FIG. 2. Quasi-periodic hyperbolic trajectory $\boldsymbol{x}_{(q)}$ for $\varepsilon = 1$ as defined by (17) on time interval $[0, 4\pi]$.

$$\boldsymbol{x}_{(q)}(t) = \begin{pmatrix}0\\0\\0\end{pmatrix} + \varepsilon\begin{pmatrix}\sin t\\ \cos\omega t + \cos t\\ \cos 2t\end{pmatrix} \quad (17)$$

where $\omega = \sqrt{2}$. An example of the trajectory (17) is shown in Fig. 2. While we use periodic and quasi-periodic examples of $\boldsymbol{x}(t)$ for illustrative purposes, boundedness of $\boldsymbol{x}(t)$ is the only requirement for our theory to hold. We have already computed the necessary control velocity for the periodic trajectory. By applying (10), (12) and (13) we find the control velocity for the quasiperiodic trajectory to be

$$\boldsymbol{v}^{(1)}_{(q)}(\boldsymbol{x},t) = \begin{pmatrix}(1-\sigma)\cos t + \sigma(\sin t - \cos\omega t)\\ -\omega\sin\omega t - (\rho - z + 1)\sin t + x\cos 2t + \cos\omega t + \cos t\\ -2\sin 2t - y\sin t - x(\cos\omega t + \cos t) + \beta\cos 2t\end{pmatrix},$$

$$\boldsymbol{v}^{(2)}_{(q)}(\boldsymbol{x},t) = \begin{pmatrix}0\\ -\sin t\cos 2t\\ \sin t(\cos\omega t + \cos t)\end{pmatrix},\ \boldsymbol{v}^{(3)}_{(q)}(\boldsymbol{x},t) = \begin{pmatrix}0\\0\\0\end{pmatrix}.$$

For a numerical analysis of the proposed control strategy, we use the third-order approximation for the periodic case. We test different values of $\varepsilon \in (0,1]$. Verifying the control strategy by numerical integration is unfeasible due to trajectory instabilities, and so we use a set-oriented approach [74] to numerically determine hyperbolic trajectories resulting from adding our control velocities $\boldsymbol{v}_{(p,q)}$ to (14). In particular, we consider a small neighborhood of the desired trajectory in the extended phase space and cover it by little 4D grid elements. For these computations we use the software package GAIO [74] and MATLAB. Based on short-time numerical integration (over time intervals of length 0.05) with respect to many initial conditions in these compact sets we obtain a directed graph that encodes transitions between grid elements. Obviously, paths in this graph correspond

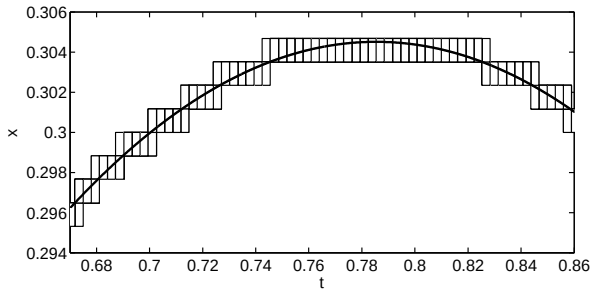

FIG. 3. A zoom in on Fig. 1 to show the numerical grid element method for determining the hyperbolic trajectories.

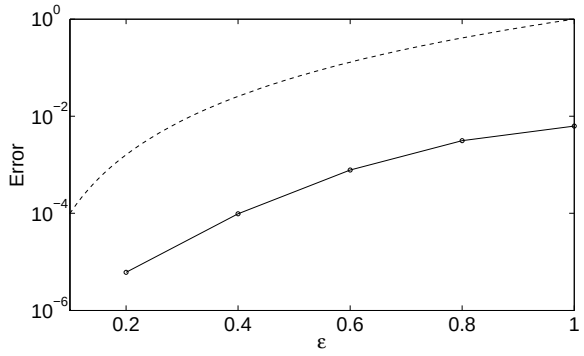

FIG. 4. Error estimates in dependence on ε for the periodic case. Box side lengths of the numerical approach outlined in the main text (solid line) compare well to theoretical order of approximation of ε^4 (dashed line).

to approximate solutions of the respective controlled differential equation. For the periodic case one is interested in closed paths, which is analogous to considering chain recurrent sets as in [74], while for the quasi-periodic case, we search for a directed path on the time span $[0, 4\pi]$.

An illustration of the computational approach is shown in Fig. 3, which zooms into the x-component of the periodic solution of Fig. 1; figures produced through this process are indistinguishable from Fig. 1 at the same scale. In Fig. 4, we show that the desired hyperbolic trajectory is indeed achieved with an accuracy of $\mathcal{O}(\varepsilon^4)$ as predicted by the theory.

We note that since third-order and higher terms vanish in the quasi-periodic example, inserting $\boldsymbol{v}_{(q)} = \varepsilon \boldsymbol{v}^{(1)}_{(q)} + \varepsilon^2 \boldsymbol{v}^{(2)}_{(q)}$ into (2) gives *exactly* the velocity field that possesses the hyperbolic trajectory $\boldsymbol{x}_{(q)}$. Indeed, we find that even with a choice of $\varepsilon = 1$ the desired trajectory is rendered up to an accuracy of 10^{-4}. The control strategy is therefore highly effective. While we have shown examples with periodicity and quasi-periodicity here, we emphasise that the numerical scheme, like the theory, does not require either condition. More details on the numerical approach will be outlined in a forthcoming manuscript.

IV. DROPLET FLOW

As microdroplets become increasingly relevant for manipulating single-cells, controlling their transport characteristics is attracting much interest. A common spherical configuration is the Hadamard-Rybczynski solution for Stokes flows [31, 32, 35, 36, 66], whose kinematic structure is similar to the classical Hill's spherical vortex [75–85] for Euler flows with an additive solid rotation. Particle trajectories of this flow satisfy

$$\dot{x} = zx - \omega_z y\,,\ \dot{y} = zy + \omega_z x\,,\ \dot{z} = 1 - 2r^2 + z^2\,, \quad (18)$$

where $r^2 = x^2 + y^2 + z^2$ and ω_z is a constant [36]. Motion is confined to level sets of the Stokes streamfunction

$$\psi(r, \theta) = \frac{1}{2} r^2 \left(1 - r^2\right) \sin^2 \theta\,, \quad (19)$$

in spherical (r, θ, ϕ)-coordinates, in each level set of which trajectories undergo an azimuthal (in ϕ) swirl of angular speed ω_z, which we shall set to 1. We note that the z-axis for $1 < z < -1$ is the one-dimensional stable manifold of the north-pole saddle fixed point $\bar{\boldsymbol{x}}_{(n)} = (0, 0, 1)^\top$, and simultaneously the one-dimensional unstable manifold of the south-pole saddle fixed point $\bar{\boldsymbol{x}}_{(s)} = (0, 0, -1)^\top$. There is no complicated transport within the system at present, and we wish to enhance transport within the sphere by having the north-pole and south-pole hyperbolic trajectories move according to our specification, chosen such that the new time-varying stable manifold of the north-pole and the time-varing unstable manifold of the south-pole intermingle in a complicated way. We therefore specify the periodic hyperbolic trajectories

$$\boldsymbol{x}_{(n)}(t) = \begin{pmatrix} 0 \\ 0 \\ 1 \end{pmatrix} + \varepsilon \begin{pmatrix} \sin t \\ \cos t \\ \sin t \cos t \end{pmatrix} \quad (20)$$

and

$$\boldsymbol{x}_{(s)}(t) = \begin{pmatrix} 0 \\ 0 \\ -1 \end{pmatrix} + \varepsilon \begin{pmatrix} \sin t \\ \sin t \cos t \\ \cos t \end{pmatrix}\,. \quad (21)$$

The first-order terms of the control velocities for the north- and the south-poles are then given by

$$\boldsymbol{v}^{(1)}_{(n)}(\boldsymbol{x}, t) = \begin{pmatrix} 2\cos t - z \sin t - x \cos t \sin t \\ -2 \sin t - z \cos t - y \cos t \sin t \\ \cos 2t + 4x \sin t + 4y \cos t + 2z \cos t \sin t \end{pmatrix}$$

and

$$\boldsymbol{v}^{(1)}_{(s)}(\boldsymbol{x}, t) = \begin{pmatrix} \cos t - z \sin t + \cos t \sin t - x \cos t \\ \cos 2t - \sin t - z \cos t \sin t - y \cos t \\ -\sin t + 4x \sin t + 4y \cos t \sin t + 2z \cos t \end{pmatrix}\,,$$

respectively. As we want to achieve the two different orbits simultaneously, we have to make sure that the two different controls act only locally, i.e. in the vicinity of the

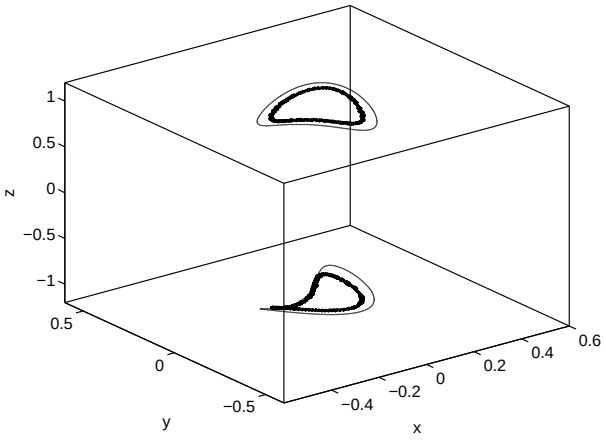

FIG. 5. Two periodic hyperbolic trajectories in (x, y, z)-space for $\varepsilon = 0.2$ as defined by (20) and (21) parametrised over time interval $[0, 2\pi]$. The thin solid curves represent the desired motion. The thick curves with smaller radius correspond to the numerically approximated trajectories based on the controlled system (22).

north and south-pole hyperbolic stagnation points only. We therefore choose Gaussians

$$g_n(\boldsymbol{x}) = e^{-10(x^2+y^2+(z-1)^2)}$$

and

$$g_s(\boldsymbol{x}) = e^{-10(x^2+y^2+(z+1)^2)}$$

and obtain the controlled system

$$\dot{\boldsymbol{x}} = \boldsymbol{u}(\boldsymbol{x}) + \varepsilon \left(g_n(\boldsymbol{x}) \boldsymbol{v}^{(1)}_{(n)}(\boldsymbol{x}, t) + g_s(\boldsymbol{x}) \boldsymbol{v}^{(1)}_{(s)}(\boldsymbol{x}, t) \right), \quad (22)$$

where $\boldsymbol{u}(\boldsymbol{x})$ denotes the right hand side of (18).

In the following we choose $\varepsilon = 0.2$ and approximate the two hyperbolic periodic orbits of the controlled system (22) using the set-oriented approach described in the previous example. These are shown in Fig. 5 together with the prescribed trajectories. As we have restricted to first-order accuracy and have two controls acting simultaneously, the desired and the obtained trajectories visibly differ but within the prescribed tolerance.

By perturbing system (18) to (22) the one-dimensional heteroclinic orbit on the z-axis connecting the north and south-pole stagnation points breaks up. Instead, each one-dimensional manifold emanating from the north and south hyperbolic trajectories periodically traces out tube-like entities as time evolves, see Fig. 6 (top). The intersection of these entites with the (x, y)-plane is depicted in Fig. 6 (bottom).

We designed the choice of hyperbolic trajectories (20) and (21) such that their relevant unstable and stable manifolds trace out two-dimensional surfaces which intersect nontrivially, as verified in Fig. 6. To assess and illustrate the mixing generated, we initialise particles on the

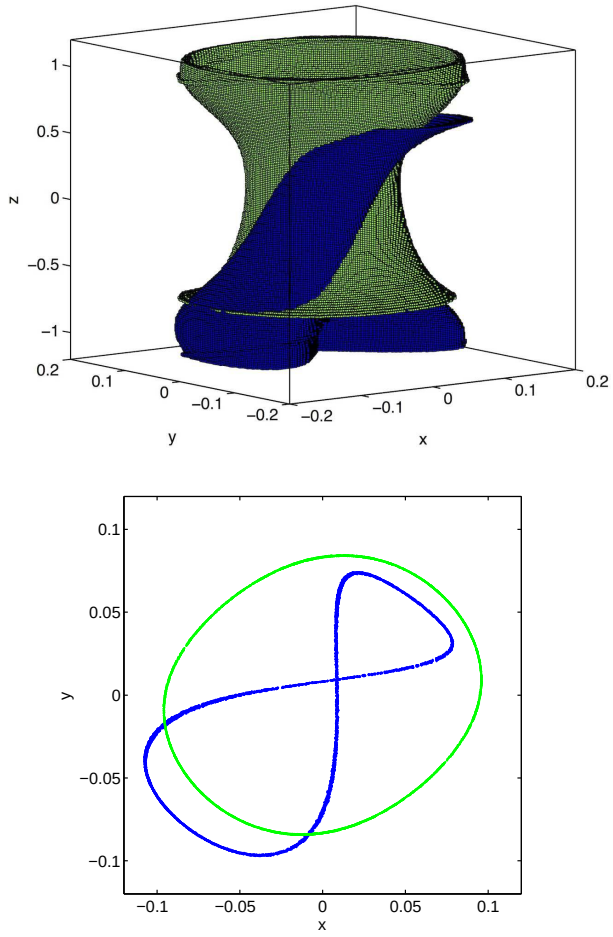

FIG. 6. (Color online) Time-trace of the stable manifold of the hyperbolic periodic orbit at the north-pole (light grey—green online) and of the unstable manifold of the hyperbolic periodic orbit at the south-pole (black—dark blue online) in (x, y, z) space (top panel) and intersection of these entities in the (x, y)-plane (bottom panel).

(x, z) and (y, z) coordinate planes and evolve them over ten periods of the flow of (22). While these planes rotate rigidly for the unperturbed flow (18), this is no longer the case for the controlled system (22). Consequently, transport and mixing is enhanced as demonstrated in Fig. 7. We remark that we have achieved global transport by applying *localised* controls at the two hyperbolic trajectories, highlighting the role hyperbolic trajectories have on the phase space. By targetting energy towards regions where it has the most impact in this fashion, we offer a new approach towards energy-constrained transport maximisation [39, 44, 49, 50]. A refinement of this idea by additionally being able to control the directions in which the stable and unstable manifolds emanate from the hyperbolic trajectory is underway.

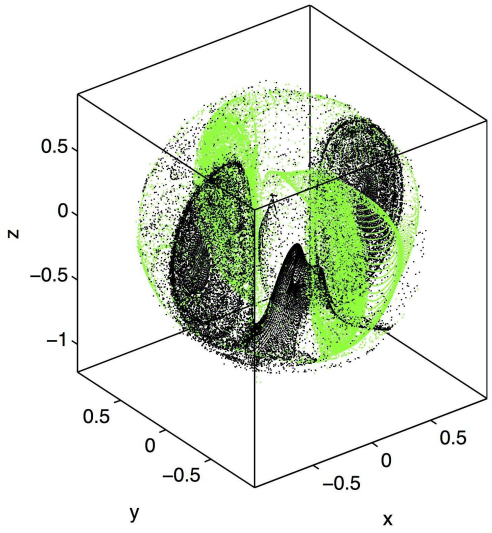

FIG. 7. (Color online) Complicated mixing structure is illustrated by advecting the coordinate planes with $x = 0$ (light grey—green online) and $y = 0$ (black) over ten periods of the forcing.

V. CONCLUDING REMARKS

In this article, we have outlined a method in which a hyperbolic trajectory of a known, potentially unsteady, system can be moved around with time as desired, by introducing a control velocity. We are able to determine the required control velocity to as high an accuracy as desired, assuming that we have full information on the uncontrolled system. For systems in which the uncontrolled velocity is specified, the computation of the control velocity is easily achieved via our equations (10), (12) and (13), as we demonstrated with an application to the Lorenz system. For fluid mechanical systems, we would similarly need to know the dominant (uncontrolled) flow to high accuracy, in order to use equations (10), (12) and (13). This we would need to have available either through an appropriate model (such as Hill's spherical vortex [27, 31, 32, 85] or the Hadamard-Rybczynski solution [35, 36, 86] if examining hyperbolic trajectories at the poles of droplets moving in an anomalous fluid), as is assumed in many fluid mechanical studies [27, 31, 35, 36, 85, e.g.]. An alternative in a purely experimental flow would be to obtain the uncontrolled velocities using PIV measurements, and then use these to impute the higher derivatives required for using our control velocity formulæ by a numerical differentiation process. The excellent accuracy we demonstrated in our analytical models in this paper will be lessened in such a situation, since the accuracy of these derivatives would be limited by the discretisation of the data. A similar approach is possible in numerically generated velocity fields.

The well-known OGY method [51, 54] is a control method which makes a system approach a fixed point which has both stable and unstable manifolds, by applying a control velocity which pushes trajectories towards the stable manifold of the fixed point. By applying our method to such a fixed point, we can first make it travel in a nonautonomous way in any fashion that we desire. A subsequent application of a 'stabilising' control on this saddle-like hyperbolic trajectory can make system trajectories approach it in the long term. Thus, our method is an addition to the chaos control literature which can generate user-specified long-term *nonautonomous* evolution of the system. For example, the Lorenz system in the chaotic regime can be made to approach $\boldsymbol{x}_{(p)}(t)$ or $\boldsymbol{x}_{(q)}(t)$ as $t \to \infty$ by applying either a form of the OGY method [51] or other methods [55, 70, e.g.] on top of the method that we have described. For $\rho < 1$, of course, a specified time-varying trajectory can be approached as $t \to \infty$ without applying the OGY method, since in this case the trajectory is attracting.

This method we have developed—which in our understanding is a first in the control of hyperbolic trajectories in n-dimensions—is a first step towards achieving a specified nonautonomous movement of specialised structures. We have shown the global impact on phase space transport as a result of controlling hyperbolic trajectories with localised controls, highlighting the significance of the method. We have moreover demonstrated remarkable accuracy of the method in idealised situations, and anticipate strong potential for implementation in realistic fluid flows or chaotic systems.

Appendix A: Definition of hyperbolic trajectory

If $\boldsymbol{u}$ in (1) were steady (autonomous), having no explicit t-dependence, an example of a hyperbolic trajectory would be a fixed point with eigenvalues bounded away from the imaginary axis. Thus, the dimensions of its stable and unstable manifolds will add to n. This understanding can be extended to *unsteady* systems, to come up with a more general definition of hyperbolicity which encapsulates all the entities enumerated in the introduction. Formally, a trajectory $\boldsymbol{x}^{(0)}(t)$ of (1) is *hyperbolic* if the $n \times n$ fundamental matrix solution $Y(t)$ of the linearised (variational) system

$$\dot{\boldsymbol{y}} = D\boldsymbol{u}\left(\boldsymbol{x}^{(0)}(t), t\right)\boldsymbol{y} \tag{A1}$$

(in which $D\boldsymbol{u}$ represents the Jacobian matrix derivative of $\boldsymbol{u}$ evaluated along the relevant trajectory $\boldsymbol{x}^{(0)}(t)$) has the property that there exist constants $\alpha_s, \alpha_u, K_s, K_u > 0$ and a projection $P : \mathbb{R}^n \to \mathbb{R}^m$ where $m \in \{0, 1, 2, \cdots, n\}$ such that the exponential dichotomy conditions [1–4]

$$\left\|Y(t)PY^{-1}(s)\right\| \leq K_s\, e^{-\alpha_s(t-s)} \text{ for } t \geq s \text{ and} \tag{A2}$$

$$\left\|Y(t)\left(\mathrm{id}-P\right)Y^{-1}(s)\right\| \leq K_u\, e^{-\alpha_u(s-t)} \text{ for } s \geq t \tag{A3}$$

are satisfied. This is a cumbersome definition, but is necessary in unsteady situations, in which instantaneous

eigenvalues are meaningless. We will give some quick intuition on this; for more detailed explanations, see [4]. If thinking of s as an initial value, (A2) indicates that initial conditions chosen in the range of P decay exponentially with rate α_s. Thus, P represents a projection on to the stable manifold of the hyperbolic trajectory. For the steady saddle point example, $-\alpha_s$ would be the real part of the stable eigenvalue which is closest to the imaginary axis. On the other hand $\mathrm{id} - P$ is a projection to the 'remainder,' which is $(n-m)$-dimensional, and (A3) ensures that there is exponential decay in forward time. This is thus a projection to the unstable manifold, and for the steady saddle example, α_u would be the real part of the unstable eigenvalue which is closest to the imaginary axis. If $m = 0$, there is no stable manifold, and the unstable manifold is n-dimensional (full-dimensional). This, as well as the situation in which $m = n$ and no unstable manifold exists, is permitted.

The definition of exponential dichotomies therefore provides for the possibility of all the entities detailed in the first paragraph of the introduction to be classified as 'hyperbolic.' The intuition is that it is *any* trajectory of a system of the form (1) (which may be autonomous or nonautonomous), which possesses full-dimensional stable and unstable manifolds.

ACKNOWLEDGMENTS

SB acknowledges with thanks grants from the Simons Foundation (#236923) and the Australian Research Council (FT130100484).

[1] W. A. Coppel, *Dichotomies in Stability Theory*, Lecture Notes Math. No. 629 (Springer-Verlag, Berlin, 1978).
[2] K. Palmer, J. Differ. Equations **55**, 225 (1984).
[3] F. Battelli and C. Lazzari, J. Differ. Equations **86**, 342 (1986).
[4] S. Balasuriya, Phys. Fluids **24**, 12710 (2012).
[5] G. Haller and A. Poje, Phys. D **119**, 352 (1998).
[6] D. Blazevski and G. Haller, Phys. D **273**, 46 (2014).
[7] A. Mancho, S. Wiggins, J. Curbelo, and C. Mendoza, Commun. Nonlin. Sci. Numer. Simu. **18**, 3530 (2013).
[8] E. Shuckburgh, in *Numerical analysis and applied mathematics (ICNAM 2012), Vols. A and B*, AIP Conference Proceedings, Vol. 1479, edited by T. Simos, G. Psihoyios, C. Tsitouras, and Z. Anastassi (AIP, 2012) pp. 650–653.
[9] G. Haller and G.-C. Yuan, Phys. D **147**, 352 (2000).
[10] I. Rypina, M. Brown, and H. Koçak, J. Phys. Oceanography **39**, 675 (2009).
[11] G. Taylor, Proc. R. Soc. Lond. A **146**, 501 (1934).
[12] B. Bentley and L. Leal, J. Fluid Mech. **167**, 219 (1986).
[13] O. Malaspinas, N. Fietier, and M. Deville, J. Non-Newtonian Fluid Mech. **165**, 1637 (2010).
[14] J. Yang and Y. Xu, Phys. Fluids **20**, 043101 (2008).
[15] J. Wintersmith, L. Zou, A. Bernoff, J. Alexander, J. Mann, E. Kooijman, and E. Mann, Phys. Rev. E **75**, 061605 (2007).
[16] J. Lee, R. Dylla-Spears, N. Teclemariam, and S. Muller, Appl. Phys. Lett. **90**, 074103 (2007).
[17] S. Hudson, F. Phelan, M. Handler, J. Cabral, K. Migler, and E. Amis, Appl. Phys. Lett. **85**, 335 (2004).
[18] S. Wereley and S. Gui, Experiments in Fluids **34**, 42 (2003).
[19] Y. Hu, D. Pine, and L. Leal, Phys. Fluids **12**, 484 (2000).
[20] A. Szeri, W. Milliken, and L. Leal, J. Fluid Mech. **237**, 33 (2006).
[21] P. Gaskell, M. Savage, and H. Thompson, J. Fluid Mech. **370**, 221 (1998).
[22] W. Xu and S. Muller, Lab Chip **11**, 435 (2011).
[23] J. Soulages, M. Oliveira, P. Souza, M. Alves, and G.H.McKinley, J. Non-Newtonian Fluid Mech. **163**, 9 (2009).
[24] S. Hu, D. LaCroix, and A. McFarland, Aerosol Sci. Tech. **43**, 311 (2009).
[25] H. Joensson and H. Svahn, Angew. Chem. Int. Ed. **51**, 12176 (2012).
[26] S.-Y. Teh, R. L. an L.-H. Hung, and A. Lee, Lab Chip **8**, 198 (2008).
[27] R. Grigoriev, Phys. Fluids **17**, 033601 (2005).
[28] M. Muradoglu and H. Stone, Phys. Fluids **17**, 073305 (2005).
[29] F. Sarrazin, T. Bonometti, L. Prat, C. Gourdan, and J. Magnaudet, Microfluid. Nanofluid. **5**, 131 (2008).
[30] K.-Y. Tung, C.-C. Li, and J.-T. Yang, Microfluid. Nanofluid. **7**, 545 (2009).
[31] R. Chabreyrie, D. Vainchtein, C. Chandre, P. Singh, and N. Aubry, Phys. Rev. E **77**, 036314 (2008).
[32] R. Chabreyrie, D. Vainchtein, C. Chandre, P. Singh, and N. Aubry, Commun. Nonlinear Sci. Numer. Simulat. **15**, 2124 (2010).
[33] M. Cordero, H. Rolfesnes, D. Burnham, P. Campbell, D. McGloin, and C. Baroud, New J. Phys. **11**, 075033 (2009).
[34] Z. Che, N.-T. Nguyen, and T. Wong, Phys. Rev. E **84**, 066309 (2011).
[35] Z. Stone and H. Stone, Phys. Fluids **17**, 063103 (2005).
[36] D. Kroujiline and H. Stone, Phys. D **130**, 105 (1999).
[37] S. Balasuriya and K. Padberg-Gehle, Phys. D **276**, 48 (2014).
[38] G. Mathew, I. Mezić, S. Grivopoulos, U. Vaidya, and L. Petzold, J. Fluid Mech. **580**, 261 (2007).
[39] Z. Lin, J.-L. Thiffeault, and C. Doering, J. Fluid Mech. **675**, 465 (2011).
[40] L. Cortelezzi, A. Adrover, and M. Giona, J. Fluid Mech. **597**, 199 (2008).
[41] A. Vikhansky, Chem. Engin. Sci. **57**, 2719 (2002).
[42] S. Balasuriya, Phys. Fluids **17**, 118103 (2005).
[43] S. Balasuriya, Phys. Rev. Lett. **105**, 064501 (2010).
[44] S. Balasuriya and M. Finn, Phys. Rev. Lett. **108**, 244503 (2012).
[45] D. Foures, C. Caulfield, and P. Schmid, J. Fluid Mech. **748**, 241 (2014).
[46] S. Balasuriya, G. Froyland, and N. Santitissadeekorn, J. Math. Anal. Appl. **409**, 119 (2014).
[47] C. Seis, Nonlinearity **26**, 3279 (2013).
[48] G. Froyland, C. González-Tokman, and T. Watson,

(2014), in preparation.
[49] O. Gubanov and L. Cortelezzi, J. Fluid Mech. **692**, 112 (2012).
[50] E. Lunasin, Z. Lin, A. Novikov, A. Mazzucato, and C. Doering, J. Math. Phys. **53**, 115611 (2012).
[51] E. Ott, C. Grebogi, and J. A. Yorke, Phys. Rev. Lett. **64**, 1196 (1990).
[52] D. Auerbach, C. Grebogi, E. Ott, and J. Yorke, Phys. Rev. Lett. **69** (1992).
[53] E. Jackson, Phys. Rev. A **44**, 4839 (1991).
[54] X. Yu, G. Chen, Y. Xia, Y. Song, and Z. Cao, IEEE Trans. Circuits Syst. I, Fundam. Theory **48**, 930 (2001).
[55] E. Tamaseviciute, G. Maikolaitis, S. Bumeliene, and A. Tamaseviciute, Phys. Rev. E **88**, 060901(R) (2013).
[56] A. Hübler and E. Lüscher, Naturwissenschaften **76**, 67 (1989).
[57] K. Pyragas, Physics Letters A **170**, 421 (1992).
[58] K. Pyragas, V. Pyragas, I. Kiss, and J. Hudson, Phys. Rev. E **70**, 026215 (2004).
[59] V. Petrov, E. Mihaliuk, S. Scott, and K. Showalter, Phys. Rev. E **51**, 3988 (1995).
[60] Y.-P. Tian, Int. J. Control **72**, 258 (1999).
[61] C. Postlethwaite and M. Silber, Phys. Rev. E **76**, 056214 (2007).
[62] J. Sieber, O. Omel'chenko, and M. Wolfrum, Phys. Rev. Lett. **112**, 054102 (2014).
[63] S. Balasuriya and K. Padberg-Gehle, SIAM J. Appl. Math. **73**, 1038 (2013).
[64] S. Boccaletti, C. Grebogi, Y. Lai, H. Mancini, and D. Maza, Phys. Reports **329**, 103 (2000).
[65] E. N. Lorenz, J. Atmos. Sci. **20**, 130 (1963).
[66] H. Stone, A. Nadim, and S. Strogatz, J. Fluid Mech. **232**, 629 (1991).
[67] $\boldsymbol{u} \in \mathrm{C}^3(\Omega)$ for each $t \in \mathbb{R}$, and $\boldsymbol{u} \in \mathrm{C}^1(\mathbb{R})$ for each $x \in \Omega$.
[68] The conditions $\boldsymbol{v} \in \mathrm{C}^3(\Omega)$ for each $(t, \varepsilon) \in \mathbb{R} \times \mathcal{I}$, $\boldsymbol{v} \in \mathrm{C}^3(\mathcal{I})$ for each $(\boldsymbol{x}, t) \in \Omega \times \mathbb{R}$, $\partial_\varepsilon^3 \boldsymbol{v}$ is bounded in $\Omega \times \mathbb{R}$, and $\boldsymbol{v} \in \mathrm{C}^1(\mathbb{R})$ for each $(\boldsymbol{x}, \varepsilon) \in \Omega \times \mathcal{I}$ are sufficient for the formulæ derived here; higher levels of smoothness will be necessary if the process is used to obtain the required velocity to higher-order.
[69] Y. Yi, J. Differ. Equations **102**, 153 (1993).
[70] K. Yagasaki, Dynamical Systems **23**, 309 (2008).
[71] See for example Theorem 11.1 in [87].
[72] Such an error bound is rigorously obtained in [63] for the first-order case in two dimensions.
[73] W. Tucker, C. R. Acad. Sci. Paris, Série I , 1197 (1999).
[74] M. Dellnitz and O. Junge (Elsevier Science, 2002) pp. 221 – 264.
[75] H. Lamb, *Hydrodynamics* (Cambridge University Press, Cambridge, 1879).
[76] J. Harper and D. Moore, J. Fluid Mech. **32** (1968).
[77] T. Laker and S. Ghiaasiaan, J. Aerosol Sci. **35**, 473 (2004).
[78] M. Shusser and D. Weihs, Fluid Dyn. Res. **42**, 025502 (2010).
[79] R. Balasubramaniam and R. Subramanian, Phys. Fluids **12**, 733 (2000).
[80] T. Sapsis and G. Haller, Chaos **20**, 017515 (2010).
[81] H. Lomeli and R. Ramirez-Ros, SIAM J. Appl. Dyn. Sys. **7**, 1527 (2008).
[82] J. Angilella and J. Brancher, Phys. Fluids **15**, 261 (2003).
[83] M. Branicki and S. Wiggins, Phys. D **238**, 1625 (2009).
[84] M. Budišić and I. Mezić, Phys. D **241**, 1255 (2012).
[85] S. Balasuriya, I. Mezić, and C. Jones, Phys. D **176**, 82 (2003).
[86] J. Hadamard, C.R. Acad. Sci. Paris **152**, 1735 (1911).
[87] P. Kloeden and M. Rasmussen, *Nonautonomous dynamical systems* (American Mathematical Society, 2011).